American Mineralogist, Volume 67, pages 1012–1020, 1982

Hyalotekite, a complex lead borosilicate: its crystal structure and the lone-pair effect of Pb(II)

Paul Brian Moore, Takaharu Araki

Department of the Geophysical Sciences
The University of Chicago
Chicago, Illinois 60637

and Subrata Ghose

Department of Geological Sciences
University of Washington
Seattle, Washington 98195

Abstract

Hyalotekite, *ca.* $Pb_2Ba_2Ca_2[B_2(Si_{1\,1/2}Be_{1/2})Si_8O_{28}]F$, Z = 2, $a = 11.310(2)$, $b = 10.955(2)$, $c = 10.317(3)$Å, $\alpha = 90.43(2)°$, $\beta = 90.02(2)°$, $\gamma = 90.16(2)°$, space group $I\bar{1}$ from Långban, Sweden was determined by Patterson and Fourier techniques, and refined to $R = 0.060$ for 3713 independent reflections. The calculated density of 3.829 g cm^{-3} based on the detailed chemical analysis by Lindström, is in good agreement with the observed specific gravity of 3.82.

Twenty-six independent atoms occur in the asymmetric unit. Two sets: Pb(1), Ba(1); and Pb(2), Ba(2) are associated spatially in pairs. Pb^{2+} and Ba^{2+} are separated by *ca.* 0.5Å, a possible segregation from the parent $I2/m$ structure due to the $6s^2$ lone-pair effect on Pb^{2+}. The structure has three principal linked components: $^{0}_{\infty}[Si_4O_{12}]$ four-membered rings, $^{0}_{\infty}[B_2(Si_{3/2}Be_{1/2})O_{12}]$ four-membered rings and $[Ca_2Pb_4O_{26}F]$ clusters. The tetrahedra link to form an incomplete framework of composition $^{3}_{\infty}[T_6O_{14}]$ ($4T_6 = BeB_4Si_{19}$ in the unit cell) which remotely resembles that of the feldspars.

Mean polyhedral distances are $^{[8]}$Pb(1)–O = 2.804, $^{[9]}$Ba(1)–O = 2.929, $^{[8]}$Pb(2)–O = 2.804, $^{[9]}$Ba(2)–O = 2.937, $^{[8]}$Ca–O = 2.437, $^{[4]}$Si(1) (= $Si_{3/4}Be_{1/4}$)–O = 1.597, $^{[4]}$Si(2)–O = 1.611, $^{[4]}$Si(3)–O 1.613, $^{[4]}$Si(4)–O = 1.610, $^{[4]}$Si(5)–O = 1.613 and $^{[4]}$B–O = 1.496Å. The F^- anion at the origin bonds to four $(Pb,Ba)^{2+}$ and two Ca^{2+}.

The hyalotekite structure has a remote structural kinship with that of gillespite, $BaFeSi_4O_{10}$.

Introduction

Hyalotekite is a rare mineral species, first named by Nordenskiöld (1877). It was subsequently studied in more chemical detail by Lindström (1887), but since then neither structure type, space group nor cell parameters have been reported. Nordenskiöld named it from the Greek *hyalos* and *tektos* owing to its property of forming a clear, colorless glass upon heating.

We expressed a special interest in hyalotekite for several reasons. First, the relatively large blocky masses from the only reported locality, Långbanshyttan, Sweden, much resemble feldspars. Second, an analysis which expressed the presence of major Pb^{2+}, Ba^{2+}, Ca^{2+}, K^{1+}, Be^{2+}, B^{3+}, Si^{4+}, O^{2-} and F^- suggested an unusual crystal–chemical problem. The senior author was attracted to the species because of its relatively high content of Pb^{2+}, and the lone-pair effect expected for this cation in an oxide environment. In addition, its curious property of easily melting to a glass attracted our attention.

The refined crystal structure demonstrated that no simple end-member formula could be written for the compound and what we suggest for such a formula is a mere approximation. Furthermore, Lindström's analysis is demonstrated to be a rather good chemical description of the species, and it appears that all subsequent chemical approximations in the literature were erroneous in some ways.

0003–004X/82/0910–1012$02.00

Table 1. Hyalotekite: chemical analysis

	1	2	3
Na_2O	0.17	---	0.082
K_2O	0.89	---	0.280
BeO	0.75	0.81	0.445
MgO	0.09	---	0.033
CaO	7.82	7.30	2.068
MnO	0.29	---	0.061
CuO	0.09	---	0.016
BaO	20.08	19.95	1.942
PbO	25.11	29.04	1.669
B_2O_3	3.73	4.53	1.598
Al_2O_3	0.18	---	0.052
Fe_2O_3	0.06	---	0.012
SiO_2	39.47	37.13	9.746
F	0.99	1.24	0.773
Cl	0.06	---	0.025
Ign	0.59	---	---
Total	100.37	100.00	46.802

[1]Lindström (1887) analysis.

[2]Computed for $Pb_2Ba_2Ca_2[B_2(Si_{1\frac{1}{2}}Be_{\frac{1}{2}})Si_8O_{28}]F$. The computed density for this composition is 3.99 g cm^{-3}.

[3]Atoms based on $\Sigma O = 28$ and analysis of column 1. The computed density for this total is 3.829 g cm^{-3}.

Hyalotekite is a new structure type, a borosilicate–fluoride of lead, barium and calcium, remotely related to the feldspar group of minerals, and to the barium iron silicate, gillespite.

Experimental

Several specimens labelled hyalotekite were examined and one sample from the Smithsonian Institution (NMNH No. 114716) was selected for the detailed structure study. We thank Mr. Paul E. Desautels for a portion of this sample. Mr. Pete Dunn, also from the U.S. National Museum, has analyzed a portion of the same hyalotekite using an electron microprobe. He has informed us that hyalotekite fluoresces a light brownish-orange in short wave ultraviolet radiation and the average value for the specific gravity is 3.82 determined on four grains. Since Dunn's observations are in good agreement with the more complete analysis of Lindström (1887), we do not list his partial results. The calculated density for the "ideal formula" and cell volume of our crystal is 3.99 g cm^{-3} based on $2\{Pb_2Ba_2Ca_2[B_2(Si_{1\,1/2}Be_{1/2})Si_8O_{28}]F\}$. However, if we calculate density on the basis of Lindström's total analysis, the value is 3.829 g cm^{-3}, in remarkably good accord with the chemical results. Computing the formula unit on the basis of this analysis, and grouping cations according to decreasing ionic radius, we get

$$(K_{0.280}Ba_{1.942}Pb_{1.669}Ca_{2.068}Na_{0.082})_{\Sigma=6.041}$$
$$(Mn^{2+}_{0.061}Mg_{0.033}Cu^{2+}_{0.016}Fe^{3+}_{0.012}Al_{0.052}Si_{0.191}B_{1.598})_{\Sigma=1.963}$$
$$(Si_{1.555}Be_{0.445})_{\Sigma=2.000}Si_8O_{28.000}(F_{0.775}Cl_{0.025})_{\Sigma=0.800}$$

The minor amounts of Mn^{2+}, Cu^{2+} and Fe^{3+} possibly represent impurities since these cations are too large for the sites into which they were apportioned. Clearly, our aforementioned "ideal formula" is only an approximate interpretation of the complex chemical nature of this species. Lindström's (1887) analysis, a calculated oxide weight percentage for the "ideal formula" and atoms in the formula unit appear in Table 1.

A single crystal fragment was ground into a sphere of diameter 0.12 mm, which was used for the X-ray intensity data collection on the computer-assisted Syntex $P\bar{1}$ diffractometer. The unit cell dimensions and the orientation matrix were determined from 15 reflections with 2θ between 20° and 35°. The intensities were measured by the θ–2θ method utilizing graphite-monochromatized Mo$K\alpha$ radiation and a scintillation counter. Variable scans were used, the minimum scan rate being 2° min^{-1} at 50 kV and 20 mA. All reflections within a 2θ limit of 60° were measured within a hemisphere assuming the space group to be $P\bar{1}$. Intensity distributions on the diffractometer and on several precession photographs suggest a triclinic (pseudomonoclinic) cell. The measured intensities were corrected for Lorentz, polarization and absorption factors. The intensities of reflections $(h + k + l) \neq 2n$ were all found to be within $3\sigma(I)$, where $\sigma(I)$ is the standard deviation of the measured intensity as determined by counting statistics. Hence, these reflections were eliminated from the data set and the space group was assumed to be $I\bar{1}$, which was subsequently confirmed by the structure determination. The refined cell parameters are a = 11.310(2)Å, α = 90.43(2)°, b = 10.955(2)Å, β = 90.02(2)°, c = 10.317(3)Å, γ = 90.16(2)°, space group $I\bar{1}$, Z = 2.

Although classical Patterson methods gave the broad structural features and the gross structural architecture was deciphered, the large, heavy cat-

Table 2. Hyalotekite: atomic coordinate parameters†

	Final $I\bar{1}$ coordinates (R = 0.060)				I2/m refinement (R = 0.23)			
	M	x	y	z	x	y	z	atom; equipoint
Pb(1)	0.290(7)	0.1543(2)	0.1726(2)	0.0043(2)	0.173	0.183	0.008	Pb
Ba(1)	0.710	0.1878(4)	0.1924(3)	0.0109(2)				
Pb(2)	0.291(7)	0.8460(3)	0.1719(2)	0.0046(2)	0.827	0.183	0.008	Pb; $\bar{x}$, y, z
Ba(2)	0.709	0.8097(3)	0.1927(2)	0.0105(2)				
Ca	1.000	0.9996(1)	0.0031(1)	0.2289(1)	0	0.002	0.229	Ca
Si(1)	0.81(1)	0.3172(2)	0.4995(2)	0.0001(2)	0.317	½	0	Si(1)
Be	0.19							
Si(2)	1.00	0.1936(2)	0.5267(2)	0.2482(2)	0.194	0.527	0.248	Si(2)
Si(3)	1.00	0.8061(2)	0.5274(2)	0.2480(2)	0.806	0.527	0.248	Si(2); $\bar{x}$, y, z
Si(4)	1.00	0.9994(2)	0.3222(2)	0.2626(2)	0	0.324	0.263	Si(4)
Si(5)	1.00	0.0002(2)	0.7224(1)	0.2825(2)	0	0.724	0.283	Si(5)
B	1.00	0.4999(7)	0.3367(6)	0.0305(7)	½	0.337	0.031	B
O(1)	1.00	0.8845(4)	0.6385(4)	0.3068(4)	0.884	0.640	0.308	O(1)
O(2)	1.00	0.8833(5)	0.4043(4)	0.2314(5)	0.882	0.400	0.228	O(2)
O(3)	1.00	0.1159(5)	0.4031(5)	0.2325(5)	0.118	0.400	0.228	O(2); $\bar{x}$, y, z
O(4)	1.00	0.1158(4)	0.6365(4)	0.3062(4)	0.116	0.640	0.308	O(1); $\bar{x}$, y, z
O(5)	1.00	0.2328(4)	0.5685(4)	0.1035(4)	0.232	0.568	0.102	O(5)
O(6)	1.00	0.7666(4)	0.5700(4)	0.1031(4)	0.768	0.568	0.102	O(5); $\bar{x}$, y, z
O(7)	1.00	0.6078(4)	0.4054(4)	0.0791(4)	0.609	0.403	0.079	O(7)
O(8)	1.00	0.3935(4)	0.4044(4)	0.0796(4)	0.391	0.403	0.079	O(7); $\bar{x}$, y, z
O(9)	1.00	0.5020(5)	0.2126(4)	0.0868(5)	½	0.216	0.084	O(9)
O(10)	1.00	0.4994(4)	0.6660(4)	0.1133(4)	½	0.664	0.110	O(10)
O(11)	1.00	0.0007(4)	0.7836(4)	0.1428(4)	0	0.781	0.143	O(11)
O(12)	1.00	0.9988(4)	0.2082(4)	0.1657(4)	0	0.210	0.167	O(12)
O(13)	1.00	0.3020(4)	0.5075(4)	0.3424(4)	0.301	0.509	0.342	O(13)
O(14)	1.00	0.6973(4)	0.5083(4)	0.3422(4)	0.699	0.509	0.342	O(13); $\bar{x}$, y, z
F	1.00	0.0000	0.0000	0.0000	0	0	0	F

†Estimated standard errors refer to the last digit. M is for the population parameters.

ions such as Pb^{2+} and Ba^{2+} presented problems. Fourier syntheses indicated a broad football-shaped maximum at what was initially believed to be a single site. In the early stages, it was assumed that Pb^{2+} and Ba^{2+} formed a solid solution. Difference Fourier syntheses eventually resolved this problem, revealing that the site was split into two partly occupied sites coupled to each other in a reciprocal fashion and separated from each other by ~0.5Å. At this stage, the structural features were clear and the framework appeared to be monoclinic with space group *I2/m*. Refinement in this space group converged to $R = 0.23$ for 2025 reflections. Admittedly, significant differences existed for many "equivalent" reflections in *I2/m*, but these were nevertheless averaged to obtain the data set for the monoclinic refinement.

The structure was then refined in space group *I1*, doubling the list of non-equivalent reflections. With split heavy atom positions, $R = 0.062$ for the converged refinement. During that refinement, it was clear that one silicon position was partly occupied by a lighter element, probably Be^{2+}, and the B^{3+} position also appeared on another position on a Fourier map. At this stage, it was noted that all atom positions could be arranged in pairs, and that each pair was related by the inversion center. Due to such parameter correlations, it is surprising that the structure refined at all in *I1*. Refining the averaged positions, now in space group $I\bar{1}$, led to $R = 0.060$ for 3713 independent reflections, where

$$R = \frac{\Sigma ||F_o| - |F_c||}{\Sigma |F_o|}.$$

Refinement minimized $w(F_o - F_c)^2$. The variables refined included the scale factor, the isotropic sec-

Table 3. Hyalotekite: anisotropic thermal vibration parameters†

Atom	U_{11}	U_{22}	U_{33}	U_{12}	U_{13}	U_{23}
Pb(1)	39(9)	124(6)	89(5)	-86(5)	-12(5)	-23(4)
Ba(1)	467(13)	257(8)	123(4)	182(7)	54(6)	32(4)
Pb(2)	122(10)	115(6)	100(5)	108(5)	6(5)	-17(4)
Ba(2)	401(11)	232(7)	129(4)	-116(7)	-67(6)	24(4)
Ca	95(7)	69(6)	94(6)	11(5)	-3(5)	7(4)
Si(1)	100(13)	156(11)	99(10)	11(8)	-10(7)	-16(7)
Si(2)	85(9)	108(8)	145(8)	9(6)	-2(7)	-4(6)
Si(3)	100(9)	98(8)	141(8)	17(6)	0(7)	-5(6)
Si(4)	128(9)	86(8)	124(8)	2(6)	-11(7)	-6(6)
Si(5)	122(9)	82(8)	104(8)	10(6)	-5(6)	-5(6)
B	203(41)	115(33)	101(30)	20(28)	10(28)	8(25)
O(1)	259(30)	205(25)	192(24)	-93(21)	-9(21)	-37(20)
O(2)	283(32)	249(28)	365(31)	98(23)	-15(25)	-81(23)
O(3)	309(33)	214(27)	363(31)	-114(23)	58(25)	-42(23)
O(4)	236(29)	193(24)	192(24)	115(20)	-15(21)	-25(19)
O(5)	187(26)	152(22)	158(22)	43(18)	4(19)	26(18)
O(6)	197(27)	172(23)	178(23)	-41(19)	-28(20)	8(19)
O(7)	207(27)	179(23)	129(21)	7(19)	-9(19)	-8(18)
O(8)	204(27)	192(24)	91(20)	22(19)	2(18)	-9(17)
O(9)	546(40)	164(25)	143(23)	-17(24)	-12(24)	4(19)
O(10)	178(25)	71(20)	177(22)	9(17)	-4(19)	-14(16)
O(11)	226(28)	165(23)	133(22)	-2(19)	-18(19)	16(18)
O(12)	168(25)	121(21)	109(20)	19(17)	-4(18)	-6(17)
O(13)	95(23)	204(24)	174(23)	28(18)	4(18)	11(18)
O(14)	156(25)	202(24)	153(22)	-41(19)	13(19)	11(18)
F	267(35)	266(31)	152(27)	26(25)	22(24)	3(23)

†Coefficients in the expression exp-[$U_{11}h^2 + U_{22}k^2 + U_{33}\ell^2 + 2U_{12}hk + 2U_{13}h\ell + 2U_{23}k\ell$]. Estimated standard errors refer to the last digit. The coefficients are each $\times 10^4$.

ondary extinction factor ($1.5(2) \times 10^{-7}$), 75 atomic coordinate parameters, 3 site occupancy parameters and 216 anisotropic thermal vibration parameters, giving a total of 296 parameters, or an independent data to variable parameter ratio of 12.5:1. Scattering curves for Pb^{2+}, Ba^{2+}, Ca^{2+}, Be^{2+}, Si^{4+} and O^{-1} were obtained from International Tables (1974) and anomalous dispersion corrections for all heavier metals from Cromer and Liberman (1970).

Table 2 lists the refined atomic coordinate parameters, Table 3 the anisotropic thermal vibration parameters, Table 4 the ellipsoids of vibration and their equivalent isotropic temperature factors (note the non-positive definite value for Pb(1)), Table 5 the bond distances and angles and Table 6 the observed and calculated structure factors.[1]

Description of the structure

The atomic arrangement of hyalotekite is rather complex. The structural description is divided into three parts: (1) the network topology, (2) the ordering of cations over the tetrahedral positions and (3) the structural distortion due to the lone-pair effect of Pb^{2+}, which has $6s^2$ in its valence electron shell. The chemical analysis of hyalotekite by Lindström (1887) is in very good agreement with the refined structure, which will be subsequently discussed in more detail.

[1]To obtain a copy of Table 6, order Document AM-82-208 from the Business Office, Mineralogical Society of America, 2000 Florida, N.W., Washington, D.C. 20009. Please remit $1.00 in advance for the microfiche.

(1) *The network topology*. The parent structure of hyalotekite belongs to space group *I2/m* and possesses 17 atoms in the asymmetric unit. As discussed before, the real space group for our crystal is $I\bar{1}$, a derivative of the parent structure. For purposes of comparison, the previously refined coordinates of the monoclinic holosymmetric group are included in Table 2. The $I\bar{1}$ structure has 26 atoms in its asymmetric unit. Proceeding from *I2/m* to $I\bar{1}$, the two (Pb,Ba) split into 4 non-equivalent atoms and Si(2), O(1), O(2), O(5), O(7) and O(13) each split into 2 non-equivalent atoms, yielding 9 additional independent positions. The Pb and Ba appear to be segregated in a coupled relationship, this separation being only about 0.5Å. This is believed to be a lone-pair effect, which is discussed later. Deviations from *I2/m* symmetry are small, as can be seen in Table 2.

The structure of hyalotekite is based on an incomplete framework of corner-linked oxygen tetrahedra. Here, we symbolized the tetrahedral cation by T. The underlying structural principle is shown as a polyhedral diagram down [001] in Figure 1. A dominant feature is the occurrence of ${}^{0}_{\infty}[Si_4O_{12}]$ four-membered rings, which are nearly in the {001} plane, approximately positioned at $z \sim 1/4, 3/4$. Such a ring involves the Si(2)-, Si(3)-, Si(4)- and Si(5)-oxygen tetrahedra. The structure is somewhat reminiscent of the feldspars with a connection of four- and eight-membered rings. However, there are some major differences. In hyalotekite, the eight-membered ring is not planar but puckered, which can be written as –Si(5)–O(4)–Si(2)–O(5)–Si(1)–O(7)–B–O(10)–Si(5)–O(4)–Si(2)–O(5)–Si(1)–O(7)–B–O(10)–. The network topology for a feldspar type four-membered ring is *uudd*, where *u* and *d* symbolize the disposition of the out-of-plane vertices, being either up (= *u*) or down (= *d*). The scapolite structure, which also contains 4- and 8-membered rings, is based on *uuuu* (*dddd*) and *udud* rings. Hyalotekite differs in two respects with regard to these structures. First, the topology is *uddd* (*uuud*). Second, the in-plane vertices which bridge to adjacent rings in feldspar and scapolite, are not linked to other tetrahedral units. Thus, O(11), O(12), O(13) and O(14) are not bridging oxygens and these define the incompleted nature of the tetrahedral framework.

Another four-membered tetrahedral ring occurs

Table 4. Hyalotekite: parameters for the ellipsoids of vibration†

Atom	i	μ_i	θ_{ia}	θ_{ib}	θ_{ic}	Beq (Å²)	Atom	i	μ_i	θ_{ia}	θ_{ib}	θ_{ic}	Beq (Å²)
Pb(1)		··········non-positive definite··········				0.67(3)	O(3)	1	0.117(10)	57(8)	34(6)	89(6)	2.34(10)
								2	0.174(9)	57(9)	110(8)	140(10)	
								3	0.213(8)	51(7)	116(5)	50(10)	
Ba(1)	1	0.107(2)	92(2)	94(4)	8(1)	2.22(4)	O(4)	1	0.099(11)	129(6)	39(5)	84(12)	1.63(9)
	2	0.124(2)	120(14)	29(46)	90(4)			2	0.137(9)	103(10)	92(11)	166(9)	
	3	0.239(3)	31(1)	61(1)	82(1)			3	0.182(8)	138(6)	129(5)	78(8)	
Pb(2)	1	0.028(15)	133(2)	44(2)	80(3)	0.88(3)	O(5)	1	0.107(10)	64(14)	143(12)	64(20)	1.30(8)
	2	0.101(2)	100(2)	85(3)	169(3)			2	0.127(9)	62(20)	102(21)	149(21)	
	3	0.150(2)	135(2)	134(2)	86(2)			3	0.148(8)	40(18)	55(11)	74(18)	
Ba(2)	1	0.106(2)	76(1)	86(2)	15(2)	2.01(3)	O(6)	1	0.117(10)	51(12)	46(24)	72(28)	1.44(8)
	2	0.132(2)	66(1)	27(1)	100(2)			2	0.130(9)	97(22)	60(27)	150(23)	
	3	0.219(3)	151(1)	63(1)	79(1)			3	0.156(8)	140(11)	59(12)	67(15)	
Ca	1	0.080(4)	72(8)	158(7)	77(8)	0.68(2)	O(7)	1	0.112(10)	84(13)	81(19)	11(17)	1.36(8)
	2	0.098(3)	106(90)	108(25)	155(90)			2	0.134(9)	102(37)	13(28)	98(20)	
	3	0.099(3)	155(73)	102(35)	69(90)			3	0.145(9)	167(37)	100(37)	83(14)	
Si(1)	1	0.094(6)	52(28)	84(10)	39(25)	0.93(6)	O(8)	1	0.095(11)	92(10)	84(10)	6(12)	1.28(8)
	2	0.102(6)	40(27)	108(8)	125(27)			2	0.134(9)	127(29)	37(29)	96(12)	
	3	0.127(4)	100(7)	161(7)	74(6)			3	0.148(9)	143(31)	126(28)	88(8)	
Si(2)	1	0.091(5)	17(90)	108(14)	90(6)	0.89(3)	O(9)	1	0.119(10)	89(4)	97(52)	7(48)	2.25(10)
	2	0.104(4)	107(14)	160(14)	98(10)			2	0.128(10)	93(4)	172(59)	97(52)	
	3	0.121(3)	93(6)	98(10)	8(10)			3	0.234(8)	177(3)	86(4)	88(3)	
Si(3)	1	0.091(4)	133(12)	42(12)	86(6)	0.89(3)	O(10)	1	0.083(12)	94(9)	8(9)	83(9)	1.12(7)
	2	0.107(4)	137(12)	131(13)	98(13)			2	0.132(9)	138(90)	87(17)	132(90)	
	3	0.119(3)	93(11)	99(10)	9(12)			3	0.136(9)	132(90)	98(10)	43(90)	
Si(4)	1	0.092(4)	89(10)	10(13)	81(10)	0.89(3)	O(11)	1	0.112(10)	81(11)	110(22)	21(19)	1.38(8)
	2	0.107(4)	131(17)	82(12)	138(17)			2	0.130(9)	99(18)	159(24)	108(22)	
	3	0.117(4)	139(17)	95(7)	49(17)			3	0.152(9)	167(14)	83(17)	78(12)	
Si(5)	1	0.089(4)	100(9)	14(9)	80(14)	0.81(3)	O(12)	1	0.103(10)	95(27)	61(65)	29(68)	1.05(7)
	2	0.101(4)	109(16)	83(15)	160(16)			2	0.109(10)	109(19)	35(56)	119(70)	
	3	0.112(4)	158(15)	102(8)	73(16)			3	0.132(9)	160(20)	108(17)	85(15)	
B	1	0.099(15)	92(26)	111(90)	20(87)	1.10(11)	O(13)	1	0.094(12)	168(19)	77(9)	89(12)	1.24(8)
	2	0.106(16)	77(17)	156(82)	109(90)			2	0.131(8)	88(13)	75(25)	165(25)	
	3	0.144(14)	13(20)	79(17)	84(15)			3	0.146(8)	78(8)	20(23)	75(25)	
O(1)	1	0.108(11)	59(7)	43(7)	64(12)	1.74(9)	O(14)	1	0.110(10)	139(18)	117(12)	62(25)	1.35(8)
	2	0.144(9)	69(10)	74(11)	153(12)			2	0.127(9)	114(22)	102(19)	152(26)	
	3	0.183(8)	38(7)	128(7)	83(9)			3	0.151(8)	121(11)	31(20)	89(15)	
O(2)	1	0.124(10)	124(8)	38(6)	74(6)	2.36(10)	F	1	0.122(11)	101(12)	89(12)	11(12)	1.80(10)
	2	0.175(9)	137(10)	107(10)	128(11)			2	0.157(10)	132(34)	42(34)	98(14)	
	3	0.208(8)	113(10)	122(6)	42(11)			3	0.170(10)	44(33)	41(35)	83(11)	

†i = ith principal axis, μ_i = rms amplitude, θ_{ia}, θ_{ib}, θ_{ic} = angles (deg.) between the ith principal axis and the cell axes a, b and c. The equivalent isotropic thermal vibration parameter, Beq, is also listed. Estimated standard errors in parentheses refer to the last digit.

in the structure, approximately situated at $z \sim 0$, ½. This ring, however, does not share the u,d-type configuration since two opposing tetrahedra in the ring are oriented with the z-axis nearly coinciding with a pseudo-$\{\bar{4}\}$ axis through a pair of tetrahedral edges. This tetrahedron is approximately $[Si_{3/4}Be_{1/4}]O_4$ in composition. The remaining non-equivalent tetrahedron is a $[BO_4]$ tetrahedron. For this ring, all oxygen vertices are linked to other tetrahedra in the structure. The formal composition of this ring would be ${}^{0}_{\infty}[B_2(Si_{3/4}Be_{1/2})O_{12}]$. The entire tetrahedral incomplete framework would have the composition ${}^{3}_{\infty}[T_6O_{14}]$, where $4T_6 = BeB_4Si_{19}$, which is the tetrahedral cation content of the unit cell. The two non-equivalent tetrahedral four-membered rings link through O(5), O(6), O(9), and O(10).

Perhaps the most striking feature of hyalotekite is its structural relationship with gillespite, $BaFe[Si_4O_{10}]$. The gillespite structure consists of sheets comprised of 4- and 8-membered rings; the four-membered rings enclose Fe^{2+} and the 8-membered rings house Ba^{2+}, which is in distorted cubic coordination and thus belongs to a coordination polyhedron of order eight (Pabst, 1943). No cations occur within the hyalotekite 4-membered rings. In addition, the ${}^{0}_{\infty}[Si_4O_{12}]$ ring is *uuud*, while in gillespite it is *uuuu*. The corrugated sheets parallel to the {001} plane are metrically similar. In hyalotekite $a \sim b \sim$

Table 5. Hyalotekite: cation–anion bond distances†

Pb(1)		Pb(2)		Ba(1)		Ba(2)	
Pb(1)-O(11)$^{(1)}$	2.375(5)	Pb(2)-O(11)$^{(1)}$	2.356(5)	Ba(1)-O(14)$^{(2)}$	2.657(5)	Ba(2)-O(13)$^{(2)}$	2.658(5)
-O(12)	2.457(5)	-O(12)	2.424(5)	-O(11)$^{(1)}$	2.674(6)	-O(12)	2.674(5)
-O(14)$^{(2)}$	2.501(5)	-O(13)$^{(2)}$	2.493(5)	-O(13)$^{(3)}$	2.675(5)	-O(11)$^{(1)}$	2.676(6)
-F	2.553(2)	-O(14)$^{(3)}$	2.579(5)	-O(12)	2.677(5)	-O(14)$^{(3)}$	2.684(5)
-O(13)$^{(3)}$	2.591(5)	-F	2.585(3)	-O(6)$^{(1)}$	2.904(5)	-O(5)$^{(1)}$	2.923(5)
-O(6)$^{(1)}$	3.155(5)	-O(5)$^{(1)}$	3.201(5)	-F	2.971(4)	-F	3.039(4)
-O(1)$^{(2)}$	3.333(6)	-O(4)$^{(2)}$	3.325(6)	-O(1)$^{(2)}$	3.125(6)	-O(4)$^{(2)}$	3.089(5)
-O(3)	3.470(6)	-O(2)	3.465(6)	-O(8)	3.334(6)	-O(2)	3.334(6)
Average	2.804	Average	2.804	-O(3)	3.345(6)	-O(7)	3.360(6)
				Average	2.929	Average	2.937
-Ca	3.441(3)	-Ca	3.457(3)				
-Ba(1)	0.439(3)	-Ba(2)	0.476(2)	-Si(3)$^{(2)}$	3.523(2)	-Si(2)$^{(2)}$	3.492(2)
						-O(9)	3.580(7)

B		Si(1) (= $Si_{3/4}Be_{1/4}$)		Si(2)		Si(3)	
B-O(9)	1.483(8)	Si(1)-O(7)$^{(1)}$	1.568(5)	Si(2)-O(13)	1.582(5)	Si(3)-O(14)	1.581(5)
-O(10)$^{(1)}$	1.484(8)	-O(8)	1.595(5)	-O(3)	1.610(5)	-O(1)	1.610(5)
-O(7)	1.507(9)	-O(6)$^{(1)}$	1.604(5)	-O(5)	1.624(5)	-O(2)	1.626(5)
-O(8)	1.509(8)	-O(5)	1.623(5)	-O(4)	1.629(5)	-O(6)	1.634(5)
Average	1.496	Average	1.597	Average	1.611	Average	1.613

Ca		Si(4)		Si(5)	
Ca-O(12)	2.344(4)	Si(4)-O(12)	1.593(5)	Si(5)-O(11)	1.594(5)
-O(14)$^{(3)}$	2.346(5)	-O(9)$^{(3)}$	1.602(5)	-O(1)	1.609(5)
-F	2.361(1)	-O(3)	1.609(5)	-O(10)$^{(3)}$	1.621(5)
-O(13)$^{(3)}$	2.366(5)	-O(2)	1.636(5)	-O(4)	1.630(5)
-O(10)$^{(3)}$	2.476(4)	Average	1.610	Average	1.613
-O(8)$^{(3)}$	2.514(5)				
-O(7)$^{(3)}$	2.533(5)				
-O(11)	2.557(5)				
Average	2.437				
-B$^{(3)}$	3.028(7)				

†Estimated standard errors in parentheses refer to the last digit. The equivalent positions (referred to Table 2) are designated as superscripts and are (1) = -x, -y, -z; (2) = ½+x, ½+y, ½+z; (3) = ½-x, ½-y, ½-z.

11.13Å, while in gillespite, it is $a\sqrt{2} \sim 10.60$Å. It is tempting to speculate that a gillespite-related phase, such as $PbFeSi_4O_{10}$ or gillespite itself, may exist at Långban, coexisting with hyalotekite.

The remaining atoms are (Pb,Ba), Ca and F. The Ca atoms are situated along the 00z line above and below F at the inversion center which joins to 2Ca, and 4(Pb,Ba) atoms. The (Pb,Ba) atoms are located within the large distorted eight-membered rings much like the alkaline earth atoms in feldspar.

(2) *The ordering of cations over tetrahedral positions*. The four-ring involving Si(2)–Si(5) at $z \sim 1/4$ appears to possess a fully ordered occupancy of $[SiO_4]$ tetrahedra by Si^{4+} exclusively. The large differences in radii and/or atomic numbers among $^{[4]}Be^{2+}$(0.27Å) and $^{[4]}B^{3+}$(0.12Å); and $^{[4]}Si^{4+}$ (0.26Å) make refinement of site populations for these atoms possible. Throughout this study, we used the values of Shannon and Prewitt (1969) for effective ionic radii. For an effective radius of $^{[2]}O^{2-}$ = 1.35Å, the interatomic distance averages would be $^{[4]}$Be–O = 1.62Å, $^{[4]}$B–O = 1.47Å and $^{[4]}$Si–O = 1.61Å. Interatomic distances listed in Table 5 are in good accord with these values. The averages $^{[4]}$Si(2)–O = 1.61, $^{[4]}$Si(3)–O = 1.61, $^{[4]}$Si(4)–O =

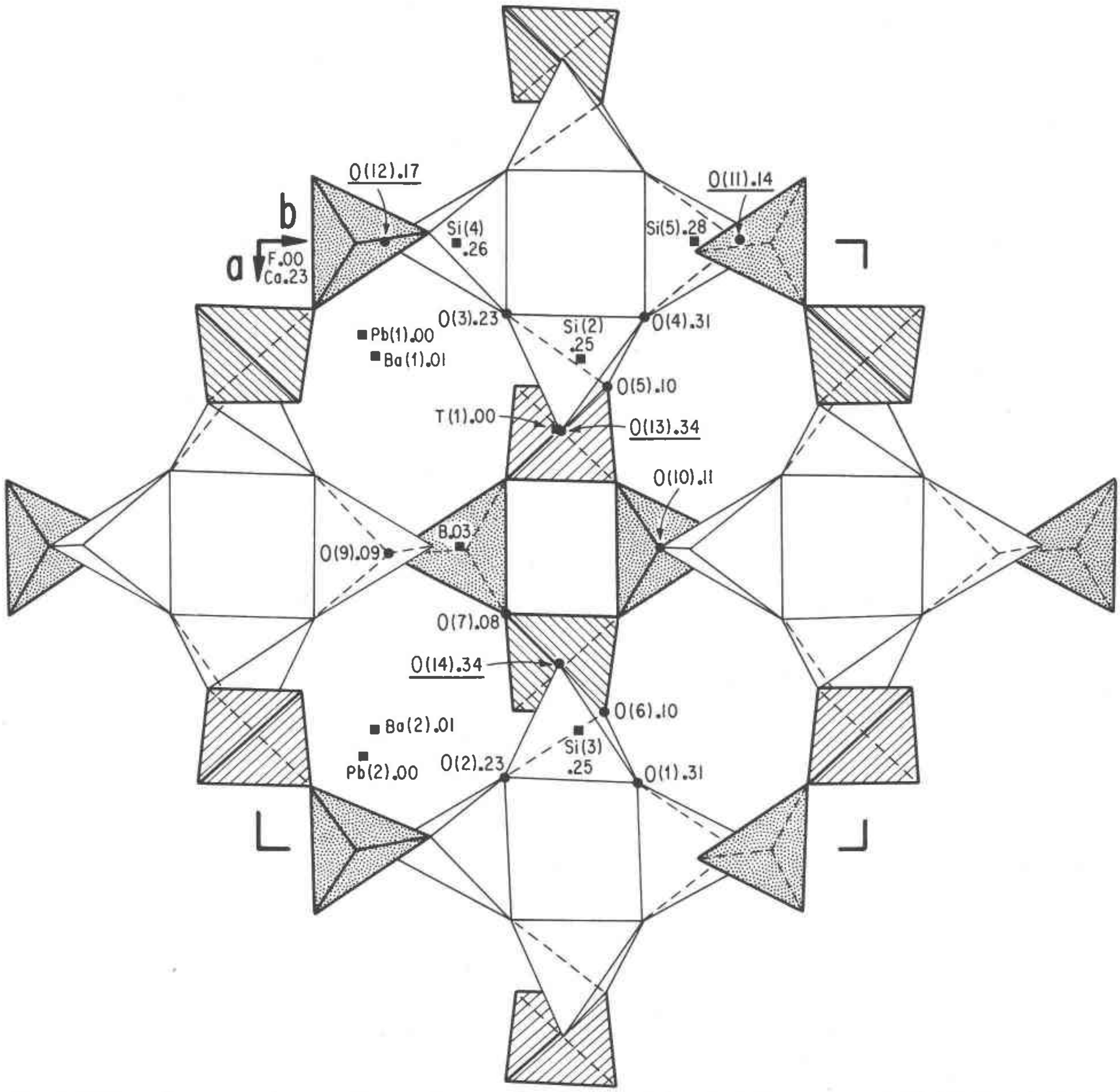

Fig. 1. Polyhedral representation of hyalotekite down [001]. The section O $\leq z \leq$ ½ is shown. The $[Si_4O_{12}]$ ring is not shaded, the T(1) (= $Si_{3/4}Be_{1/4})O_4$ tetrahedra are ruled and the BO_4 tetrahedra are stippled. Heights are given as fractional coordinates in z. The asymmetric unit in Table 2 is labelled. Terminal oxygens are underlined.

1.61 and $^{[4]}$Si(5)–O = 1.61Å are in excellent agreement with the anticipated average. The value $^{[4]}$B–O = 1.50Å is only slightly larger than the expected value. The value $^{[4]}$Si(1)–O = 1.60Å, where Si(1) ~ $Si_{3/4}$ $Be_{1/4}$ is only slightly smaller than the expected average for these two cations. This raises the question of whether or not B^{3+} instead of Be^{2+} substitutes at this site, since these cations are practically impossible to distinguish by their X-ray scattering powers alone. However, a contradiction arises in formal charge assignment for the formula unit and, in the absence of further evidence for deciding the site population of Si(1), we prefer to write it as $Si_{3/4}Be_{1/4}$. It should be further noted that Lindström's (1887) analysis also shows the presence of this amount of BeO in the compound. The formula for the tetrahedral fraction can therefore be written $[Si_8(Si_{3/2}Be_{1/2})B_2O_{28}]$ with two such units in the unit cell.

The ellipsoids of vibration listed in Table 4 suggest that the assignments of scattering curves and the site population refinements in Table 2 are a fairly good approximation to the atoms present. If Al^{3+} or Si^{4+} were substituted for B^{3+}, we would expect a substantial decrease in the equivalent isotropic thermal parameter. On the other hand, $B_{eq} = 1.10\text{Å}^2$ for B suggests that this site corresponds to boron, or possibly even some minor site vacancies. It is possible, however, that substitution of minor Si^{4+} for B^{3+} would induce local disorder causing a subsequent increase in B_{eq}.

(3) *The structural distortion due to Pb^{2+}*. Hyalotekite is an example where Pb^{2+} with its $6s^2$ lone pair evinces a particularly noticeable effect on the entire structure. Hyalotekite's aristotype belongs to a space group with considerably higher symmetry than found in the actual structure; that is $I2/m \rightarrow I\bar{1}$. Order–disorder in the tetrahedral framework does not appear to be a cause for this, since Si(1) and B have site symmetries C_2 and C_s, respectively, and do not split into non-equivalent Si (or B) positions in the triclinic subgroup, unlike feldspar in which Al–Si ordering destroys such symmetry elements. In hyalotekite, these special positions merely become general positions, and the general positions in the aristotype split into two sets of general positions. In these general positions, there does not appear to be any evidence of ordering.

If we extract the large cations and their coordinating anions, the picture changes drastically. Figure 2 shows the $Pb(1)_2Pb(2)_2O_{20}F$ cluster, which is composed of four fused PbO_7F polyhedra (polyhedron No. 197, of Britton and Dunitz, 1973). They are roughly equivalent, and would be identical in $I2/m$. Each polyhedron shares two faces with two other polyhedra and the common F vertex is also corner-linked to the fourth polyhedron. Thus, F links to four $Pb^{2+}(Ba^{2+})$ cations, and also to two Ca^{2+} cations above and below. The CaO_7F polyhedron corresponds to polyhedron No. 127 of maximal symmetry C_s in Britton and Dunitz and shares triangular faces with the PbO_7F polyhedra. Polyhedron No. 197 can be regarded as having a square pyramidal cap with F at the vertex. In this structure, four triangular faces are shared, two with adjacent Pb^{2+} cations and two with adjacent Ca^{2+} cations.

The remarkable feature about the PbO_7F group is that all bonds to the face-sharing vertices are the shortest for their polyhedra (Fig. 2 and Table 5), while the remaining three Pb–O bonds on the opposite side of the F atom are the longest for their polyhedra. This is interpreted as the result of the lone pair-bond effect with the $6s^2$ lone pair located opposite the tightly bound F^- anion. This model is reminiscent of the arguments applied to sulfosalts in general and galena in particular (Moore, manuscript), where the lone pair–bond pair interactions lead to bond length dilation. In fact, on the bond pair side, the Pb–O distances range from 2.36 to 2.59Å. The shortest is not much larger than the effective $^{[6]}Pb^{4+}$–O = 2.18Å separation.

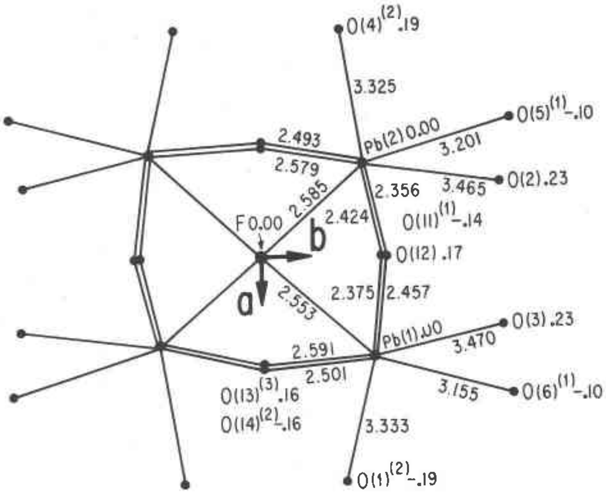

Fig. 2. Spoke diagram of the $Pb_4O_{20}F$ cluster in hyalotekite. The additional Ca above and below F at the origin are omitted (the $Ca_2Pb_4O_{26}F$ cluster). Heights are shown as fractional coordinates in z and bond distances are shown.

Pb^{2+} and Ba^{2+} are split in hyalotekite, separated by about 0.4–0.5Å. From the site population refinement (Table 2), a total of 1.162 Pb^{2+} cations occurs per 28 oxygens. However, Lindström's analysis in Table 1 indicates an aliquot of 1.669 Pb^{2+} atoms. This difference is not easily explicable, since the solid solution structural effect of a cation with a lone pair (such as Pb^{2+}) and a cation with inert gas configuration (such as Ba^{2+}) is not clear. It is also possible that some analytical error may exist in the quantitative separation of Pb and Ba. Due to the lone pair effect, the $^{[8]}Pb^{2+}$–O distances range from 2.36 to 3.47Å. The $^{[8]}Ca$–O distances range from 2.34 to 2.56Å and $^{[9]}Ba$–O from 2.66 to 3.36Å. Clearly, the most severe polyhedral distortion occurs for Pb^{2+}. Did Pb^{2+} and Ba^{2+} occur in solid solution at the crystallizing temperature of hyalotekite and then partition as the phase cooled? This is an intriguing question, since an affirmative answer would suggest that the high temperature space group would be $I2/m$ and that the lone pair effect would be temperature-dependent, at least for Pb^{2+} oxysalts. A possibility that this effect may indeed exist appears in Hurlbut (1955) where conclusive evidence showed that some wulfenites, $Pb^{2+}MoO_4$, are in fact polar, and that centrosymmetric wulfenites may themselves be merohedrally twinned on {001}. High temperature crystallographic studies of polar wulfenites and hyalotekite would be instructive.

Pb^{2+} lone pair effects

Table 5 includes only the cation–anion distances in absence of a good qualitative model for the lone pair effect on nearest bond pairs. If any prediction were to be made regarding the locus of the lone pair, it would be toward O(1), O(3), O(6) for Pb(1) and O(2), O(4) and O(5) for Pb(2) by mere inspection of the Pb^{2+}–O bond distances. These are those vertices which oppose the coordinated F^- anion, or better yet, the capped square pyramid.

Acknowledgments

P.B.M. and T.A. acknowledge the grant NSF EAR79-18259 (Geochemistry) and the Materials Research Laboratory grant (NSF) to The University of Chicago, and S.G. thanks NSF EAR76-13373 (Geochemistry) for support in this study, and P. Boving and C. Wan for assistance in data collection. We join in thanking the U.S. National Museum (Smithsonian Institution) for donation of the sample for study.

References

Britton, D. and Dunitz, J. D. (1973) A complete catalogue of polyhedra with eight or fewer vertices. Acta Crystallographica, A29, 362-371.

Cromer, D. T. and Liberman, D. (1970) Relativistic calculation of anomalous scattering factors for X-rays. Los Alamos Scientific Laboratory, University of California Report LA-4403, University of California-34.

Hurlbut, C. S., Jr. (1955) Wulfenite symmetry as shown on crystals from Jugoslavia. American Mineralogist, 40, 857–860.

International Tables for X-ray Crystallography, Vol. 4. Revised and Supplementary Tables (1974). Ibers, J. A. and Hamilton, W. C. Eds., Kynoch Press, Birmingham.

Lindström, G. (1887) Om hyalotekit från Långban. Öfversigt af Kongliga Svenska Vetenskaps-Akademiens Förhandlingar, 44, 589–593.

Nordenskiöld, A. E. (1877) Nya mineralier från Långban. Geologiska Föreningens Förhandlingar, 3, 376–384.

Pabst, A. (1943) Crystal structure of gillespite, $BaFeSi_4O_{10}$. American Mineralogist, 28, 372–390.

Shannon, R. D. and Prewitt, C. T. (1969) Effective ionic radii in oxides and fluorides. Acta Crystallographica, B25, 925–946.

Manuscript received, February 11, 1982;
accepted for publication, May 11, 1982.